Desalination and Water Treatment
www.deswater.com
doi: 10.5004/dwt.2023.29815

306 (2023) 99–111
September

Hydrothermal carbonization of agro-waste for phosphate and nitrate removal from water environment

B. Senthil Rathi[a], P. Senthil Kumar[b,*]

[a]*Department of Bioengineering, Institute of Biotechnology, Saveetha School of Engineering, SIMATS, Chennai 602105, India, email: rathisjce@gmail.com*
[b]*Centre for Pollution Control and Environmental Engineering, Pondicherry University, Chinna Kalapet, Puducherry-605014, India, email: senthilchem8582@gmail.com*

Received 8 April 2023; Accepted 26 July 2023

ABSTRACT

Worldwide, nitrate and phosphate pollution of freshwater resources is seen as a serious issue. The most pervasive pollution in an aquatic environment, eutrophication, which harms the ecology, and serious hazards to human health are all brought on by the overwhelming release of phosphate and nitrate. As a result, the elimination and restoration of such phosphate and nitrate are regarded as one of the solutions to limit the algae blooms of aquatic environment by applying a variety of techniques. Adsorption is a simple, cost-effective, green, and all-purpose technique used to clean up nitrate and phosphate from liquid waste. Utilizing greener hydrothermal carbonization technique, alkaline impregnation, and neutral atmosphere activation, we developed a unique method for producing porous carbon sphere from bagasse in this article. The produced carbon sphere demonstrates a sizable ability to extract contaminants from aqueous solutions. Outcomes of the experiments demonstrate that the optimum condition was reached in 60 min, and the ideal pH and carbon sphere dosage were discovered to be 7 and 1.4 g/L, correspondingly. The nitrate and phosphate sorption kinetics are suited by the pseudo-first-order equation with coefficient of correlation values of 0.99 and 0.98, correspondingly. Additionally, isotherm research demonstrates that Freundlich isotherms with R^2 value as 0.9978 for nitrate adsorption and 0.9975 for phosphate adsorption provided a good model for these adsorption studies.

Keywords: Carbon spheres; Phosphate removal; Nitrate removal; Agro-waste; Sugarcane bagasse; Adsorption

1. Introduction

Polluted water caused by an excessive level of fertilizers for example, nitrogen and phosphorus is a serious ecological concern all over the globe, since both organisms are involved in the eutrophication of incoming waterbodies [1,2]. For the growth of flora, mammals, and all other living things, nitrate (N) and phosphate (P) are necessary micronutrients. Farming, domestic trash, and other sectors all produce enormous amounts of P and N ions, which end up in lakes as well as other water bodies [3,4]. Surface water eutrophication is a major and worldwide threat to the environment. One of the most important essential goals of wastewater treatment is to achieve low phosphate and nitrate concentrations to minimize algae blooms [5,6]. Such generally requires the use of treatment methods such

---

[*] Corresponding author.

1944-3994/1944-3986

as nano-techniques, physical, biological, and chemical [7]. The expulsion of P and N from aqueous solution using various sorbents is frequently regarded as an effective and economic technique to enhance existing procedures [8].

The most effective approach for removing contaminants from liquids is adsorption by activated carbon. Nevertheless, there is a great need for low-cost activated carbon substances due to the expensiveness of activated carbon and the difficulties of its renewal after sorption. Consequently, sugarcane bagasse was chosen as a cheaply available bio waste source for the production of thick, fiber activated carbon for the adsorption of pollutants. By utilizing $ZnCl_2$ in an ambient thermo-chemical activation process and pyrolyzing it at varying temperatures (400°C–600°C), activated carbon made from bagasse was produced [9]. carbon spheres have grabbed people's fascination with the subject of study since they have multiple applications as adsorbent materials, catalytic support, power conversion, and power storage in lithium batteries [10]. Hydrothermal method, chemical vapour deposition, laser ablation, polymerization, plasma method, and thermal decomposition of organic compounds are all methods for producing carbon spheres [11]. Each of the methods listed above has advantages and disadvantages. Furthermore, these procedures employ chemicals as reagents for the synthesis of carbon spheres, as well as some reducing agents or catalyst as required [12].

The hydrothermal carbonization of feedstock, among many other processes, is a potential option for the synthesis of novel chemicals based on carbon with a wide range of uses [13,14]. Hydrothermal carbonization is the simultaneous dewatering and thermal decomposition of a product to increase its amount of carbon in order to attain a higher heating value [15,16]. It is accomplished by repeatedly imparting higher temperature (180°C–220°C) to feedstock held in water at excessive pressure over several hours [17,18]. Hydrothermal carbonization and steam activating for syrup color removal were used to generate biochar from bagasse. The hydrothermal carbonization temperature fluctuated from 180°C–240°C throughout a waiting time of 30–90 min, while the steaming temperature fluctuation was 700°C–900°C at 1 h. The production of dry-basis adsorbents, according to the findings, ranged from 10.4% to 27.1%. The product had a highest Brunauer–Emmett–Teller contact area of 390 m^2/g. The overall volume fraction of the adsorbents was 0.1–0.25 cm^3/g, with an average particle size of 2.2–2.5 nm [19]. The hydrothermal carbonization technique has major benefits given that it may produce a broad range of inexpensive and renewable carbon-based products with appealing nanoporous and crosslinking sequences for a variety of purposes [20].

This study focuses on the production of carbon spheres and activated carbon spheres from bagasse utilizing standard Teflon lined stainless steel autoclave that might be used to eradicate P and N from aqueous solution. Batch adsorption investigations were performed in the best possible conditions to define adsorption-affecting parameters such as adsorbent dosage, pollutant concentration and pH for determining adsorption mechanism and removal mechanism among contaminant and activated carbon spheres.

2. Materials and procedures

2.1. Adsorbate and its analytical techniques

A standard phosphate reagent was prepared by mixing 0.7165 g of 99.5% pure anhydrous potassium dihydrogen phosphate in distilled water, then diluting the mixture to 1,000 mL. In a similar manner, standard nitrate solution was obtained by dissolving autoclave 0.7218 g of 99.5% pure potassium nitrate in 1 L of distilled water according to guidelines for analyzing both water and sewage. The levels of N and P in the aqueous solution were determined using the UV testing method, which is a common method for testing both wastewater and water. For treating samples before to testing for N ion concentration, 1 mL of 1 N hydrochloric acid was mixed with 50 mL of pure supernatant, and deionized water was employed to serve as a blank for analysis. Furthermore, organic matter interference was examined through determining the absorbance of the supernatant solution at 275 nm. The specimen used for measuring the level of P in the water solution, on the other hand, was generated by first incorporating phenolphthalein indicator solution and then introducing strong acid solution until the pink colour disappeared. Each flask received 4 mL of acid-molybdate solution and was thoroughly diluted by inverting each flask four to six times. The flasks were then sealed and agitated by tilting each flask four to six times with 0.5 mL of stannous chloride solution. Lastly, after 10 min but before 12 min, the colour of P concentrate was optically measured at 690 nm employing deionized water as a blank. Utilizing an UV-Vis spectroscopy (Lark LI-UV-7000 , India) at wavelengths of 220 and 690 nm, respectively, the amounts of N and P in the aqueous solution were determined utilizing traditional technique for the investigation of wastewater and water.

2.2. Adsorbent

Residual bagasse garbage was purchased from a nearby small-scale juice shop in Chennai. A blender was used to crush and shred sugarcane bagasse into a powder form. To distinguish tiny to separate small filaments from the ultrafine dust, the fine dust was screened through mesh measuring 160 μ in size. This powder was extensively washed with water after being immersed in a 0.1 M sodium hydroxide solution at temperature of 80°C for contact time of 4 h to remove inorganic contaminants. A high-pressure autoclave made of Teflon-lined stainless steel was employed to encapsulate approximately 3 to 4 g of dry biomasses tight. The autoclave was then fired at 190°C over 14 h. A brownish-black semi-solid mixture was recovered as quickly as the process was finished and the equipment kept for cooling. Acetone, ethanol, and distilled water were used to rinse this hard chemical continually till the reddish-brown supernatant changed to a transparent permeate. Thereafter, carbon spheres were dried by vacuum at temperature range of 70°C–80°C for an entire night [21]. The characterization of the prepared adsorbent has been presented in previous work [12].

2.3. Chemical activation of carbon spheres

The potassium hydroxide impregnation technique was used to activate the carbon spheres, which were originally synthesized. The potassium hydroxide and carbon sphere mixture were then agitated regularly for about 5–6 h in a heating oven. This material without any moisture was pulverised and heated to 700°C for 2 h at a speed of 3°C/min in a N_2 environment. Nitrogen is kept moving at a speed of 10 mL/min. After the process has finished, the compound was taken out and properly rinsed with 0.1 mol/L Hydrochloric acid till the compound became neutral. The desired product was ultimately dried by air.

2.4. Batch adsorption studies

Activated carbon spheres were used in batch adsorption studies with a 100 mL P and N aqueous solution in a typical room environment. The filtrate was strained once sorption was finished, and P and N concentrations were analysed by using Ultraviolet Visible spectroscopy (Lark LI-UV-7000) at wavelengths of 220 nm and 690 nm, correspondingly. For determining the adsorption-influencing factors, such as pH, dose, initial concentration, temperature, and contact duration, a standard approach was used. The pH of ideal solution for the greatest combined eradication of P and N ions was found to be between 2 and 10, with an adsorbent dosage range of 0.2–1.8. By adjusting the intensity of P and N ions from 20 to 100 mg/L, the combined eradication of P and N ions was examined.

2.5. Thermodynamic parameters

A number of thermodynamics variables, including enthalpy ($\Delta H°$, kJ/mol), entropy ($\Delta S°$, kJ/mol), and Gibbs free energy ($\Delta G°$, kJ/mol), were used to illustrate the basic idea behind the adsorption process. The formula below may be used to determine these thermodynamics parameters. Graphically the thermodynamic parameters were computed.

$$K_c = \frac{C_{\text{ae}}}{C_e} \tag{1}$$

$$\Delta G° = -RT\ln\left(K_c\right) \tag{2}$$

$$\log K_c = \frac{\Delta S°}{2.303R} - \frac{\Delta H°}{2.303RT} \tag{3}$$

2.6. Isotherm experiments

The carbon sphere content was varied from 0.2 to 1.8 g/L for the isotherm experiment while other variables like pH 7, time 60 min, initial concentration of P and N as 20 mg/L and temperature 30°C were kept constant. The following relation was used to compute the saturation level of N and P ion sorption on carbon spheres.

$$q_e = \frac{\left(C_0 - C_e\right)}{\text{W}_{\text{sorbent}}} \times V \tag{4}$$

The Freundlich, Temkin, and Langmuir isotherms, which are shown in Table 1, were used to fit the results to the discovered equilibria. A non-linear regression study was performed using the MATLAB R2016a tool, which can be used to provide isothermal parameters such regression coefficients like root mean squared errors (RMSE), sum of squared errors (SSE), and coefficient of correlation (R^2).

2.7. Kinetics study

Adsorption kinetic measurements were performed in a conical flask of 100 mL of changing nitrate and phosphate ion concentrations (20–100 mg/L) in the vicinity of carbon spheres. The samples were shaken for 60 min. The experimental conditions where pH is 7, temperature is 30°C and adsorbent dose for P and N were 1 and 1.4 g/L, respectively. During every 10-min lag phase, samples were taken using the agitator and drained using the Whatman 42 Filter Pad. The amount of nitrate and phosphate ion associated with the carbon sphere at various times was calculated using the previous formula.

$$q_t = \frac{\left(C_0 - C_t\right)}{\text{W}_{\text{sorbent}}} \times V \tag{5}$$

Three different analytical models (i) Elovich model, (ii) pseudo-first-order and (iii) pseudo-second-order were provided (Table 2) to support the theoretical findings that were reached. A non-linear regression study was performed using the MATLAB R2016a tool, which can be used to provide isothermal parameters such regression coefficients like RMSE, SSE, and coefficient of correlation (R^2).

Table 1
Adsorption isotherms for elimination of N and P by HTC carbon spheres

Isotherm name	Model equation	References
Langmuir isotherm	$q_e = \frac{C_e K_L q_m}{1 + C_e K_L}$	[27]
Freundlich isotherm	$q_e = K_F C_e^{\frac{1}{n}}$	[28]
Temkin isotherm	$q_e = \frac{RT}{b_t}\ln\left(a_t C_e\right)$	[29]

Table 2
Adsorption kinetics for elimination of N and P by HTC carbon spheres

Kinetics	Model equation	References
Pseudo-first-order kinetic model	$q_t = q_e\left(1 - \exp\left(-k_1 t\right)\right)$	[30]
Pseudo-second-order kinetic model	$q_t = \frac{q_e^2 k_2 t}{1 + q_e k_2 t}$	[31]
Elovich model	$q_t = \frac{1}{\beta}\ln\left(\alpha\beta\right) + \frac{1}{\beta}\ln\left(t\right)$	[32]

2.8. Intraparticle diffusion model

Investigations were conducted using the intraparticle diffusion model if particle diffusion was a rate-limiting phase during nitrate and phosphate sorption onto carbon spheres [22,23]. The governing equation for the model is provided as.

$$q_t = k_p t^{1/2} \quad (6)$$

2.9. Batch adsorber design based on isotherm data

Using the presented approach, the design of a sorption method was calculated using Langmuir isotherm statistics. Because of the scarcity of substantial empirical design processes, experimental data, rely on equilibrium adsorption research are the majority often used approach of predicting the size and effectiveness of the adsorber [24]. In the single-stage procedure under equilibrium, the mass balance for phosphate and nitrate solution is stated as:

$$V\left(C_0 - C_e\right) = m\left(q_0 - q_e\right) = m\left(q_e\right) \quad (7)$$

$$\frac{m}{V} = \frac{C_0 - C_e}{q_e} \quad (8)$$

Freundlich equation from Table 1:

$$\frac{m}{V} = \frac{C_0 - C_e}{K_F C_e^{1/n}} \quad (9)$$

3. Results and discussion

3.1. pH-effect on phosphate and nitrate removal by hydrothermal carbonization carbon spheres

Fig. 1 demonstrates that while significant N eradication was attained at pH 7, strong P eradication was shown between pH 6 and 8. According to the experimental data on the impact of the pH of the starting solution, N eradication enhanced as the pH rose from 2 to 7 and then decreased after pH 7, as depicted in Fig. 1. The breakup of active sites on the surface of hydrothermal carbonization (HTC) carbon spheres is controlled by the aqueous phase pH effect, which may be the cause of this. While poor elimination below pH 7 could be ascribed to HTC carbon sphere oxides being unstable at low pH values, the decline in N eradication when pH is more than 7, which may be caused by intense compete with hydroxides. The adsorptive removal of nitrate utilising solid waste from a manufacturing at pH value of 7 and reduced elimination at pH of above 7 values produced results that are comparable to this one [24]. Contrarily, as indicated in Fig. 1, limited phosphate removal at pH less than 5 and strong phosphate elimination in the pH range 6–8 was both noted. Low phosphate elimination at pH less than 5, pH may be caused by H_3PO_4, which predominates and is poor bonds to the active sites of HTC carbon spheres. The reduced efficacy of P eradication at larger pHs may be due to competition between OH^- and $H_2PO_4^{-1}$, HPO_4^{-2}, and PO_4^{-3} for adsorption sites. Finally, it should be noted that the broad pH range for phosphate removal is crucial in terms of removing the pollutant.

3.2. Adsorbent dose impact on phosphate and nitrate removal by HTC carbon spheres

Fig. 2 shows a graph showing the ratio of phosphate and nitrate reductions vs the HTC carbon sphere dose. The graph shows that there may have been a correlation between the % of P and N eradication and the mass change of carbon sphere dose, increased when the dose of carbon spheres was increased. The percentage of phosphate and nitrate elimination increased from 33.63% to 99.62% and 21.65% to 99.31%, respectively after a change in the carbon sphere dose from 200 to 1,800 mg/L, respectively. When the ratio of carbon sphere to phosphate and nitrate is higher, there is highly quick lateral sorption to the carbon sphere surface, which results in a lower concentration of phosphate and nitrate in the solution than when it is lower. As the dosage of the adsorbent rose, the number of active binding spots and surface area expanded, which led to a rise in the % elimination. However, phosphate and nitrate absorption did not increase significantly at greater adsorbent doses, most likely

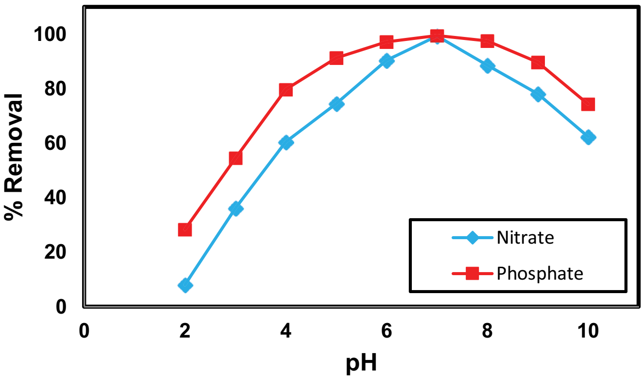

Fig. 1. Impact of pH on the adsorption of N and P by HTC carbon spheres, initial concentration of P and N: 20 mg/L, adsorbent dosage for P and N: 1 and 1.4 g/L and adsorption temperature: 30°C.

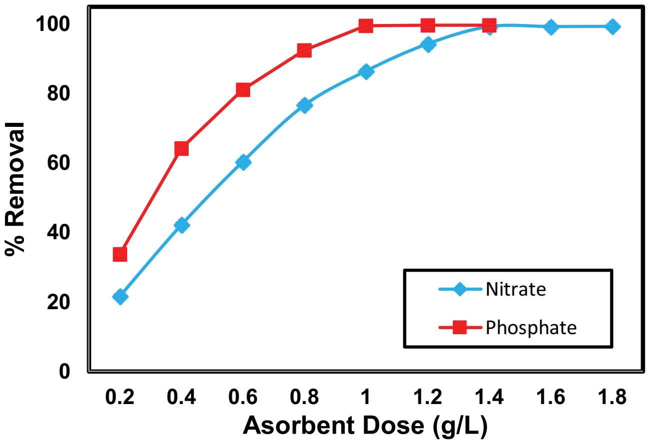

Fig. 2. Impact of adsorbent dose on the adsorption of N and P by HTC carbon spheres, initial concentration of P and N: 20 mg/L, pH: 7 and adsorption temperature: 30°C.

because exhaustion might be reached. Since a specific quantity of carbon spheres can only absorb a fixed number of particles. Therefore, the quantity of aqueous medium that may be purified with a dosage of carbon spheres increases with increasing carbon sphere dose. The percentage of phosphate and nitrate elimination raises the saturated concentration just above dose of 1.4 g/L, almost exceeding the fixed value for HTC carbon spheres, implying that 1.4 g/L is the proper dosage of carbon spheres for the elimination of P and N concentrations from synthetic wastewater.

3.3. Initial P and N concentration impact on P and N removal by HTC carbon spheres

By modifying the starting level of P and N between 20 and 100 mg/L, the impact of P and N initial concentration on elimination of P and N was examined. The starting concentration of P and N ions plays a key role in their removal, acting as a vital driving factor between the HTC carbon spheres and aqueous solution to overcome the phosphate and nitrate ion's mass transfer reluctance. With optimal conditions of 1.4 g/L of HTC carbon spheres, pH of 7, temperature at 30°C, and period of 1 h, the methodology was conducted to evaluate the influence of the starting intensity of phosphate and nitrate ions on various concentrations of P and N ions ranges from 20–100 mg/L on HTC carbon spheres. In Fig. 3 it could be noted how strength of P and N ions affects the ability of HTC carbon spheres to remove these ions. The findings demonstrate that the starting intensity of P and N ions enhanced from 20 to 100 mg/L due to ordinal quantity of HTC carbon sphere dose and the decrease in its active sites on the surface, meanwhile the percentage of eradication of phosphate and nitrate concentrations from synthetic aqueous system decreased from 99.57% to 89.41% and 99.25% to 82.63%. The reduction in phosphate and nitrate adsorption may indicate that there isn't enough space to accommodate the high starting concentration of phosphate and nitrate. Because there is greater surface area on the adsorbent for fewer adsorbate species, phosphate and nitrate are taken up greater readily at low concentrations.

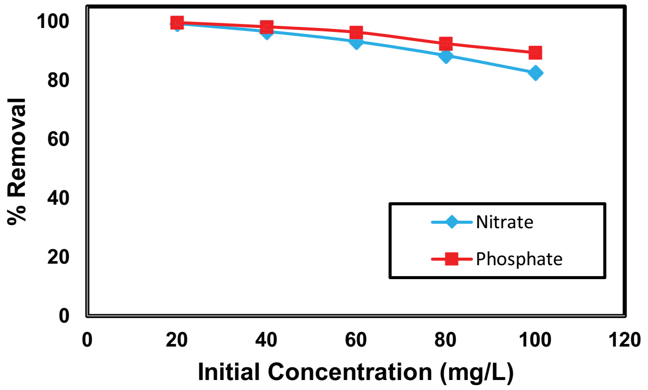

Fig. 3. Impact of initial concentration on the adsorption of N and P by HTC carbon spheres, pH: 7, adsorbent dosage for P and N: 1 and 1.4 g/L and adsorption temperature: 30°C.

3.4. Contact time impact on P and N elimination by HTC carbon spheres

Fig. 4 depicts the influence of the time on the elimination of N and P concentrations from prepared solution in the intensity level of 20–100 mg/L at pH 7 and 303 K. By adjusting the interaction duration from 10 to 90 min and enabling 100 mL of sample solution with 20–100 mg/L of nitrate and phosphate levels to be adsorbed onto 1.4 g/L carbon sphere by agitating the solution at 150 rpm, optimum condition was ascertained. The outcomes demonstrate that phosphate (Fig. 4b) and nitrate (Fig. 4a) elimination increased throughout time, peaked at 60 min, and then stabilised. Similar findings by earlier studies were confirmed, and the outcome is consistent with the removal of N and P by solid waste residue [24]. Results from transfer of N and P ions on HTC carbon spheres showed that the adsorption process gets better with longer contact times. An additional rise in contact time has a minimal impact on the proportion of nitrate and phosphate eliminated. Due to the greater surface area of the HTC carbon sphere for N and P ions, the sorption capacity of N and P removal was initially enhanced. The adsorption rate is then governed by the rate at which the N and P atoms are moved from outer pores to inner surface of carbon sphere, and the ability of HTC carbon sphere is finally exhausted when the adhered nitrate

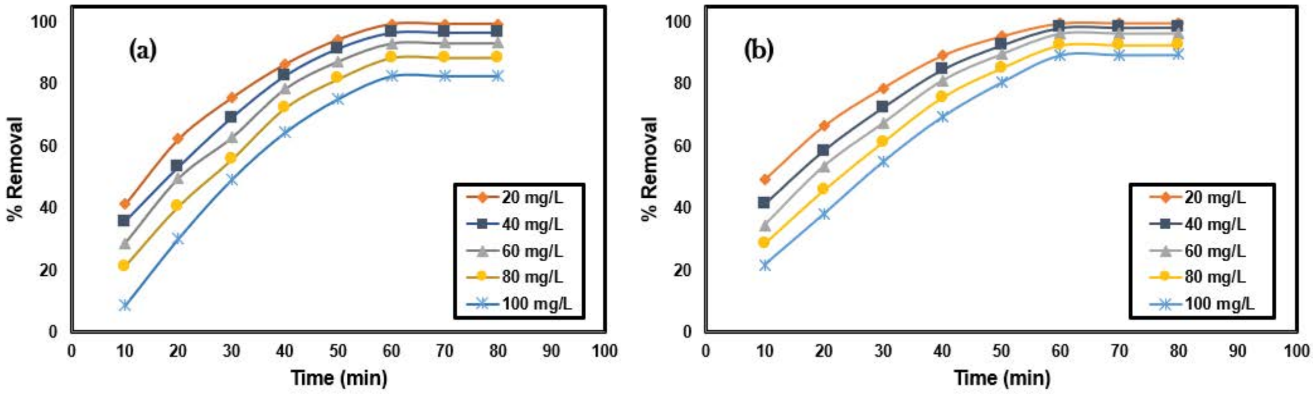

Fig. 4. Contact time impact on the adsorption of (a) nitrates and (b) phosphate by HTC, pH: 7, adsorbent dosage for P and N: 1 and 1.4 g/L and adsorption temperature: 30°C.

and phosphate ions create a single layer. Additionally, it is essential since each active site could only attach a single ion in such a single layer due to the limiting number of successful sorbent positions throughout the mechanism.

3.5. Temperature impact on P and N elimination by HTC carbon spheres

The temperature impact of the N and P ion removal on the HTC carbon spheres was accomplished in the 100 mL conical flask. With an optimum pH of 7.0, a treatment period of 60 min, and a dosage of 1.4 g/L of HTC carbon spheres, the study was performed at a temperature range between 30°C and 60°C for starting arsenic concentrations ranges 20–100 mg/L. The elimination of N decreased from 99.25% to 94.25%, 96.57% to 90.35%, 93.17% to 87.33%, 88.42% to 82.36%, and 82.63% to 76.31% with the rise in temperature from 30°C to 60°C for the starting N concentration between 20 and 100 mg/L rises by 20 accordingly (Fig. 5a). The elimination of P decreased from 99.57% to 95.78%, 98.14% to 92.33%, 96.31% to 90.47%, 92.49% to 86.31%, and 89.41% to 83.69% with the rise in temperature from 30°C to 60°C for the starting P concentration between 20 and 100 mg/L rises by 20 accordingly (Fig. 5b). This was caused by the degradation of the adsorption sites and adsorption forces between N and P on the surface of adsorbent. It shown that the adsorption process is inherently exothermic [25,26].

3.6. Study of thermodynamics under investigation

Eqs. (2) and (3) were used to calculate thermodynamic variables including enthalpy, free energy, and entropy. The values of enthalpy and entropy are determined from logk_C against inverse of temperature graph (Fig. 6). When the temperature was increased, nitrate and phosphate ion adsorption on HTC carbon sphere decreased from 30°C to 60°C, as shown in Fig. 6. The charts were utilized to evaluate the thermodynamic variables (Table 3). As a result of having negative H°, the process was quite exothermic. The negative values of Gibb's free energy show that the elimination of P and N by HTC carbon spheres is thermodynamically desirable and spontaneous. As Gibb's free energy rises as the temperature increases, indicating that N and P sorption process is more conceivable and advantageous at higher temperatures. A negative ΔS° value, on the other hand, indicates that there is less randomness at the HTC carbon spheres surface and P and N solution interface during the adsorption process. The random nature of sorption at the HTC carbon sphere-nitrate and phosphate ion interface area may be characterized using this.

3.7. Adsorption isotherms on phosphate and nitrate removal by HTC carbon spheres

The isotherm parameter can be used to analyse the interactions between nitrate and phosphate ions, HTC carbon spheres, dynamic equilibrium, and the adsorption capacity for sorption technique. The summary outcomes are shown in Table 4 for the combined elimination of both P and N utilizing HTC carbon spheres. The data were evaluated using the following generally used isotherms namely (i) Langmuir, (ii) Freundlich, and (iii) Temkin isotherms. Figs. 7 and 8 show, respectively, the isothermal fit for the eradication of N and

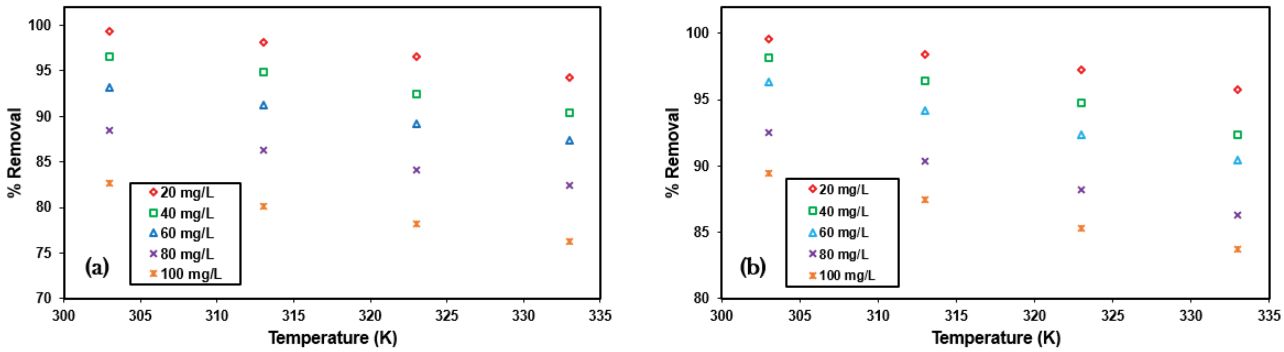

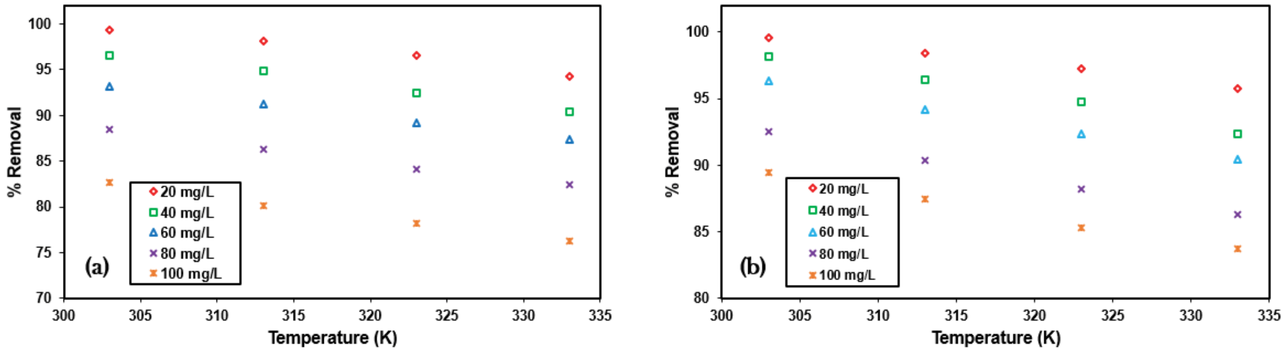

Fig. 5. Temperature impact on the adsorption of (a) nitrates and (b) phosphate by HTC, pH: 7, adsorbent dosage for P and N: 1 and 1.4 g/L.

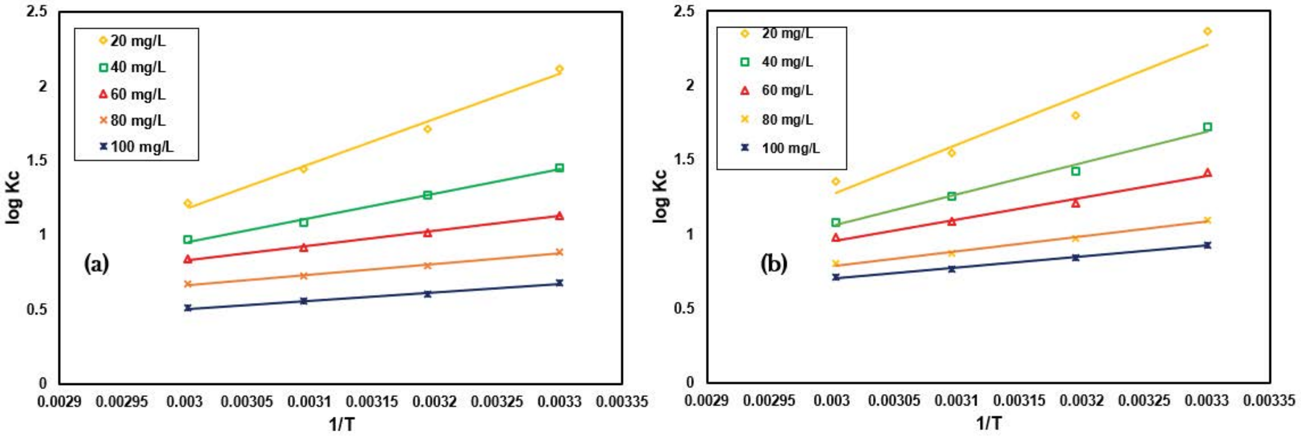

Fig. 6. Thermodynamics on the adsorption of (a) nitrates and (b) phosphate by HTC.

Table 3
Thermodynamic analysis on the N and P by HTC carbon spheres

C_o (mg/L)	$\Delta H°$ (kJ/mol)	$\Delta S°$ (J/mol·K)	$\Delta G°$ (kJ/mol)			
			303 K	313 K	323 K	333 K
Nitrates						
20	–57.978	–151.473	–12.307	–10.278	–8.931	–7.743
40	–31.228	–75.516	–8.408	–7.592	–6.724	–6.193
60	–19.205	–41.779	–6.583	–6.108	–5.664	–5.345
80	–13.866	–28.950	–5.121	–4.783	–4.469	–4.266
100	–10.802	–22.804	–3.929	–3.635	–3.438	–3.238
Phosphates						
20	–63.817	–167.135	–13.716	–10.769	–9.535	–8.644
40	–40.592	–101.576	–9.990	–8.540	–7.764	–6.888
60	–28.012	–65.809	–8.217	–7.249	–6.693	–6.231
80	–18.760	–41.186	–6.325	–5.814	–5.404	–5.098
100	–14.062	–28.740	–5.374	–5.049	–4.730	–4.528

P ions on HTC carbon spheres. The outcome demonstrated that the Freundlich isotherm, with R^2 values of 0.9978 and 0.9975, accordingly, adequately described the adsorption of nitrate and phosphate. In the same way, Temkin isotherm with R^2 is 0.9622 for phosphate and 0.9654 for nitrate, while adsorption isotherm data fitted to Langmuir isotherms have coefficient of regression of 0.9203 for phosphate and 0.9155 for nitrate. The analysis of R^2 values proved that the Freundlich model, which had a higher R^2, provided a better description of the optimum sorption with adsorption capacities of 91.23 and 60.96 mg/g for P and N, respectively. This outcome shows that the multi-layer adsorption of N and P ions is characterized and that the surface of the carbon spheres is heterogeneous. Freundlich exponent results was noted to be larger than 1 (3.373 and 3.292). It was indicated that the HTC carbon spheres are capable of removing all of the P and N ions from the prepared solution of water and that the adsorption technique used is very beneficial.

Table 4
Isotherm analysis on the removal of nitrates and phosphates by HTC

Models	Parameters	Nitrates	Phosphates
Langmuir	q_m (mg/g)	60.96	91.23
	K_L (L/mg)	0.6112	0.9895
	R^2	0.9155	0.9203
	SSE	107.9	241
	RMSE	5.998	8.964
Freundlich	K_F ((mg/g)(L/mg)$^{(1/n)}$)	25.69	43.62
	N	3.373	3.292
	R^2	0.9978	0.9975
	SSE	2.838	7.558
	RMSE	0.9727	1.587
Temkin	A (L/mg)	21.94	33.96
	B	4.08	6.141
	b (kJ/mol)	0.617	0.410
	R^2	0.9654	0.9622
	SSE	44.2	114.4
	RMSE	3.839	6.176

3.8. Adsorption kinetics on phosphate and nitrate removal by HTC carbon spheres

Kinetic analysis might be utilized to develop the kinetic conceptual model for the adsorption of N and P ions on HTC carbon spheres. Three different kinetic model namely Elovich, pseudo-first kinetic models and second-order kinetic models have been studied in the current study using the findings of empirical contact time measurements. Figs. 9 and 10 demonstrate how the kinetic findings, including the sorption of N and P ions, are adsorbed to the HTC carbon spheres. Tables 5 and 6 contain the values of the constant in kinetic model and coefficient of regression. Inferring that the adsorption mechanism conforms the pseudo-first-order kinetic system with concentration range of 20 to 100 mg/L is possible with the help of the R^2 value. It was claimed that as the value of intensity increases for phosphate, the kinetic model shifts from second-order to first order. Due to competition with the active adsorbents sites on the surface of the carbon spheres, variability in the rate constant values occur. Due to less competition for the active adsorbents sites at low N and P ion concentrations, there was a reasonably high rate of adsorption. Additionally, higher N and P ion concentrations in the synthetic aqueous solution led to a slower rate of adsorption because there is more competition for the binding sites. Table 7 represents the comparison of HTC with other adsorbent for removing nitrates and phosphates.

3.9. Diffusion mechanism on the removal of nitrates and phosphate by HTC

The chart of q_t vs. square root of time has not passes through the origin, as depicted in Fig. 11a and b, which indicates that diffusion isn't the rate-determining step in the investigation of equilibrium data using the diffusion model. The phosphate and nitrate adsorption plots just

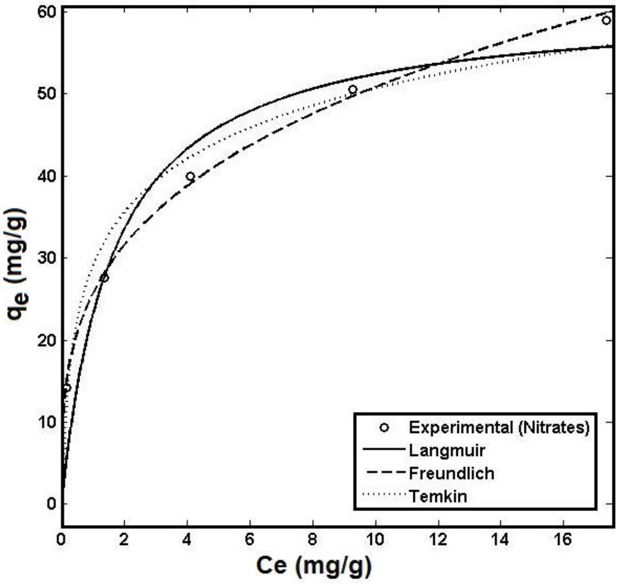

Fig. 7. Adsorption isotherms on the elimination of nitrates by HTC.

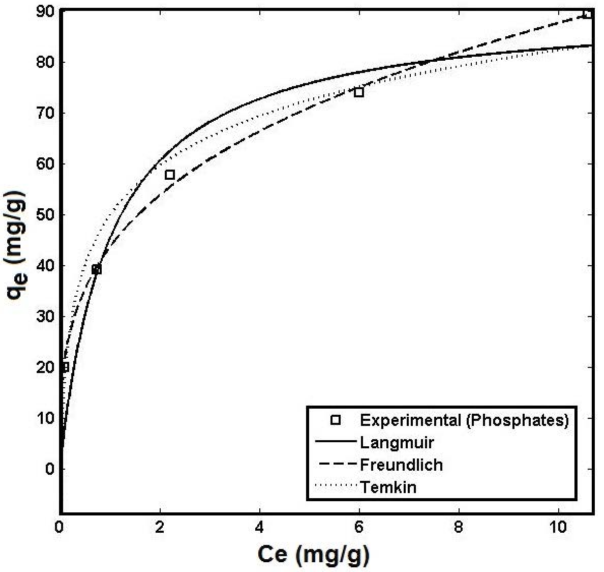

Fig. 8. Adsorption isotherms on the elimination of phosphates by HTC.

Table 5
Removal kinetics of nitrates by HTC

Models	Parameters	Nitrates				
		20 mg/L	40 mg/L	60 mg/L	80 mg/L	100 mg/L
Pseudo-first-order	$q_{e,\exp}$ (mg/g)	14.25	27.68	40.15	50.82	59.34
	k_1 (min^{-1})	0.0479	0.04005	0.03521	0.02883	0.0219
	$q_{e,\text{cal}}$ (mg/g)	14.61	29.24	43.36	57.67	73.97
	R^2	0.9925	0.9872	0.9848	0.9741	0.943
	SSE	0.5208	4.242	12.44	41.93	171.8
	RMSE	0.2728	0.7785	1.333	2.447	4.954
Pseudo-second-order	k_2 (g/mg·min)	0.002838	0.001033	0.0005479	0.0002866	0.0001355
	$q_{e,\text{cal}}$ (mg/g)	18.03	37.5	57.5	80.65	112.2
	R^2	0.9823	0.9727	0.9688	0.9591	0.931
	SSE	1.233	9.038	25.51	66.25	208
	RMSE	0.4198	1.136	1.909	3.076	5.451
Elovich	α_E	0.3915	0.06158	0.02282	0.008312	0.002628
	β_E	0.893	3.348	6.19	10.17	16.81
	R^2	0.9565	0.9515	0.9492	0.9435	0.9197
	SSE	3.033	16.02	41.5	91.68	242.2
	RMSE	0.6582	1.513	2.435	3.619	5.883

weren't straight across the whole-time interval and did not cross the origin (Fig. 11). This shows that there were other rate-limiting processes involved in the combined sorption of nitrate and phosphate (Table 8). As a result, various mass transfer mechanisms, such as bulk diffusion and film diffusion, may be associated in figuring out how N and P ions are transferred from the prepared P and N solution to adsorbent surface.

3.10. Freundlich model-based batch adsorber design

As utilized quantities of the contaminant and targeted sorption % values rose, so did the mass of HTC carbon sphere materials require. The use of 0.3–22.9 g of HTC carbon spherical material to reduce a given volume of 1–10 L with a nitrate content of 20–100 mg/L to 75%–95% is necessary (Fig. 12). The use of 0.2–13.35 g of HTC carbon spherical material to reduce a given volume of 1–10 L with a phosphate content of 20–100 mg/L to 75%–95% is necessary (Fig. 13). Relative to the other materials under study, less of the components for the carbon spheres were used. This variation was connected to the increased nitrate and phosphate adsorption performance of HTC carbon spheres.

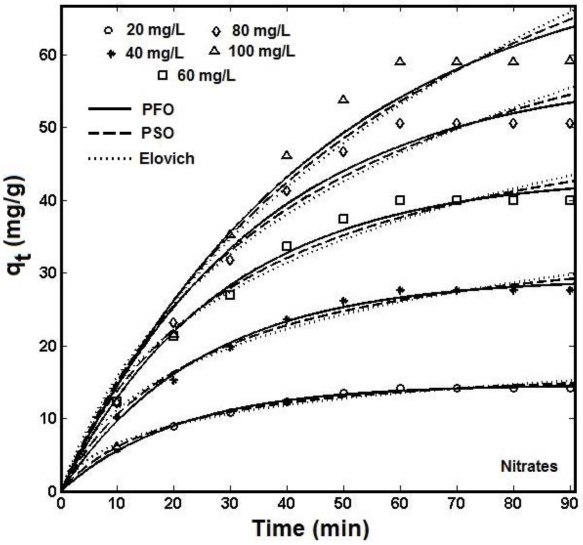

Fig. 9. Adsorption kinetics on the elimination of nitrates by HTC.

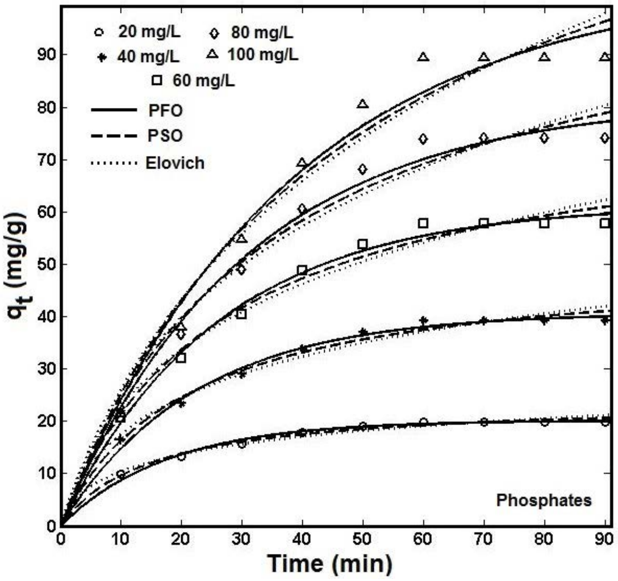

Fig. 10. Adsorption kinetics on the elimination of phosphates by HTC.

Table 6
Removal kinetics of phosphates by HTC

Models	Parameters	Phosphates				
		20 mg/L	40 mg/L	60 mg/L	80 mg/L	100 mg/L
Pseudo-first-order	$q_{e,\text{exp}}$ (mg/g)	20.2	39.52	57.95	74.25	89.75
	k_1 (min^{-1})	0.05685	0.0452	0.03881	0.03276	0.02635
	$q_{e,\text{cal}}$ (mg/g)	20.14	40.69	61.39	81.46	104.4
	R^2	0.9792	0.9862	0.989	0.9844	0.9753
	SSE	2.197	7.666	16.14	45.59	129.2
	RMSE	0.5602	1.046	1.518	2.552	4.296
Pseudo-second-order	k_2 (g/mg·min)	0.002816	0.0009336	0.0004677	0.0002595	0.0001373
	$q_{e,\text{cal}}$ (mg/g)	23.99	50.67	79.22	109.6	148.8
	R^2	0.9828	0.9794	0.9769	0.9709	0.9632
	SSE	1.819	11.45	34.07	84.71	192.3
	RMSE	0.5098	1.279	2.206	3.479	5.241
Elovich	α_E	0.5209	0.06844	0.02291	0.009208	0.0035
	β_E	1.246	4.446	8.319	13.1	20.26
	R^2	0.9577	0.96	0.9582	0.9551	0.9509
	SSE	4.461	22.28	61.52	130.9	256.7
	RMSE	0.7983	1.784	2.965	4.325	6.056

Table 7
Comparison of HTC with other adsorbent for removing nitrates and phosphates

Contaminant	Adsorbent	Adsorption capacity (mg/g)	References
Nitrate	Date palm-derived biochar	28.06	[33]
Phosphate	Date palm-derived biochar	177.97	[33]
Nitrate	HTC carbon sphere from sugarcane bagasse	60.96	Current study
Phosphate	HTC carbon sphere from sugarcane bagasse	91.23	Current study
Nitrate	Mesoporous MCM-48 silica	43	[1]
Phosphate	Mesoporous MCM-48 silica	46	[1]
Nitrate	Banana bract	73.3	[34]
Phosphate	Banana bract	87	[34]
Nitrate	AC from boron waste	63.2	[35]
Phosphate	AC from boron waste	52.5	[35]
Phosphate	Bamboo activated carbon	4.74	[36]

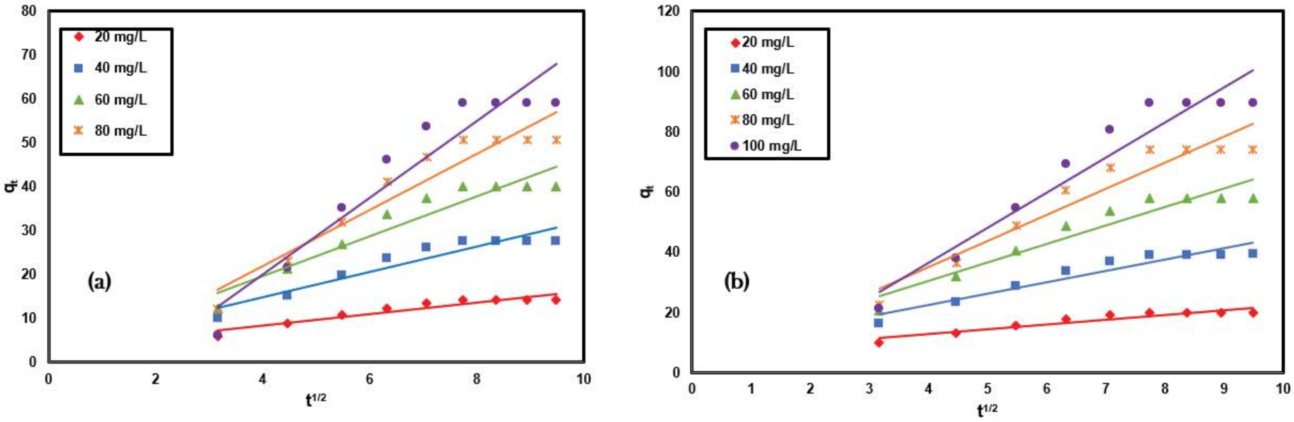

Fig. 11. Diffusion mechanism on the elimination of nitrates (a) and phosphate (b) by HTC.

Table 8
Diffusion analysis on the removal of nitrates and phosphates by HTC

Parameters	Nitrates					Phosphates				
	20 mg/L	40 mg/L	60 mg/L	80 mg/L	100 mg/L	20 mg/L	40 mg/L	60 mg/L	80 mg/L	100 mg/L
k_p	1.320	2.884	4.545	6.425	8.747	1.620	3.756	6.125	8.645	11.62
C	3.057	3.250	1.517	–3.903	–14.99	6.275	7.490	5.887	0.578	–9.765
R^2	0.896	0.903	0.906	0.913	0.910	0.893	0.909	0.913	0.920	0.928

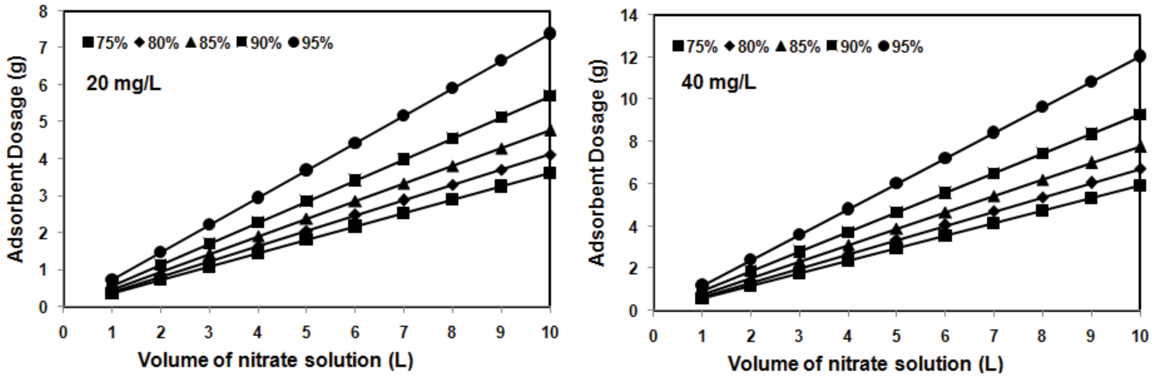

Fig. 12 (Continued)

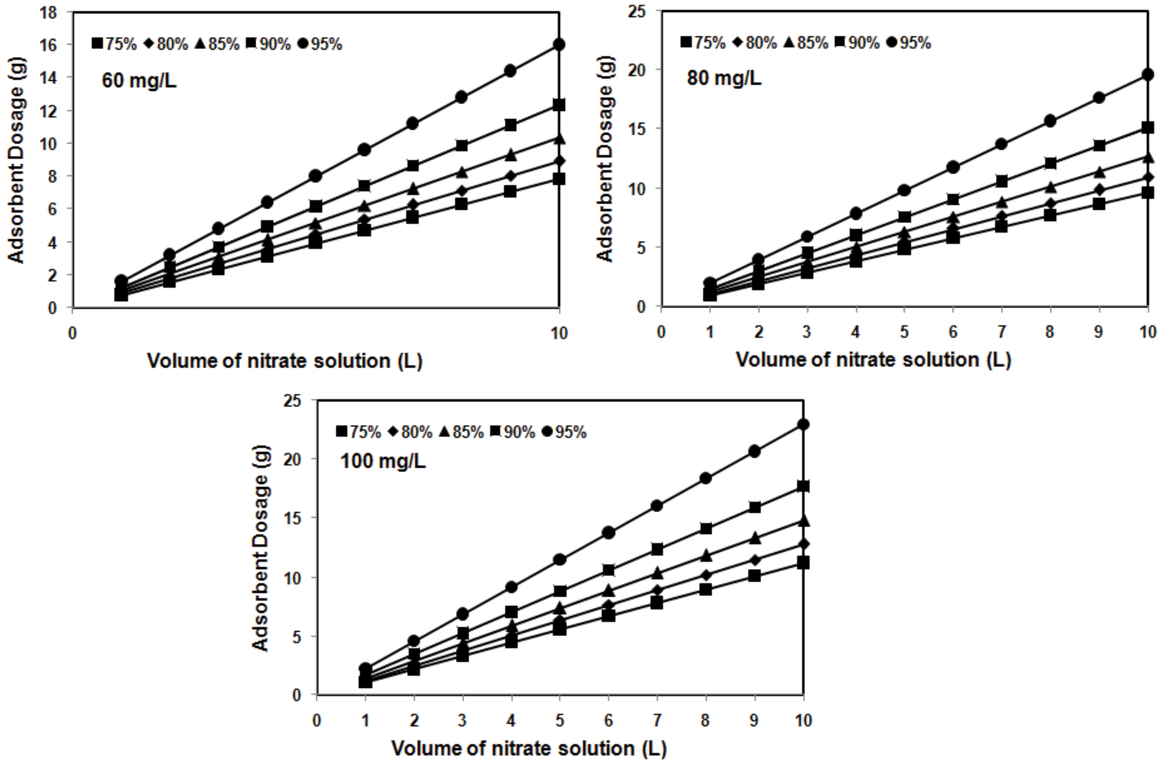

Fig. 12. Batch adsorber design on the elimination of nitrates by HTC.

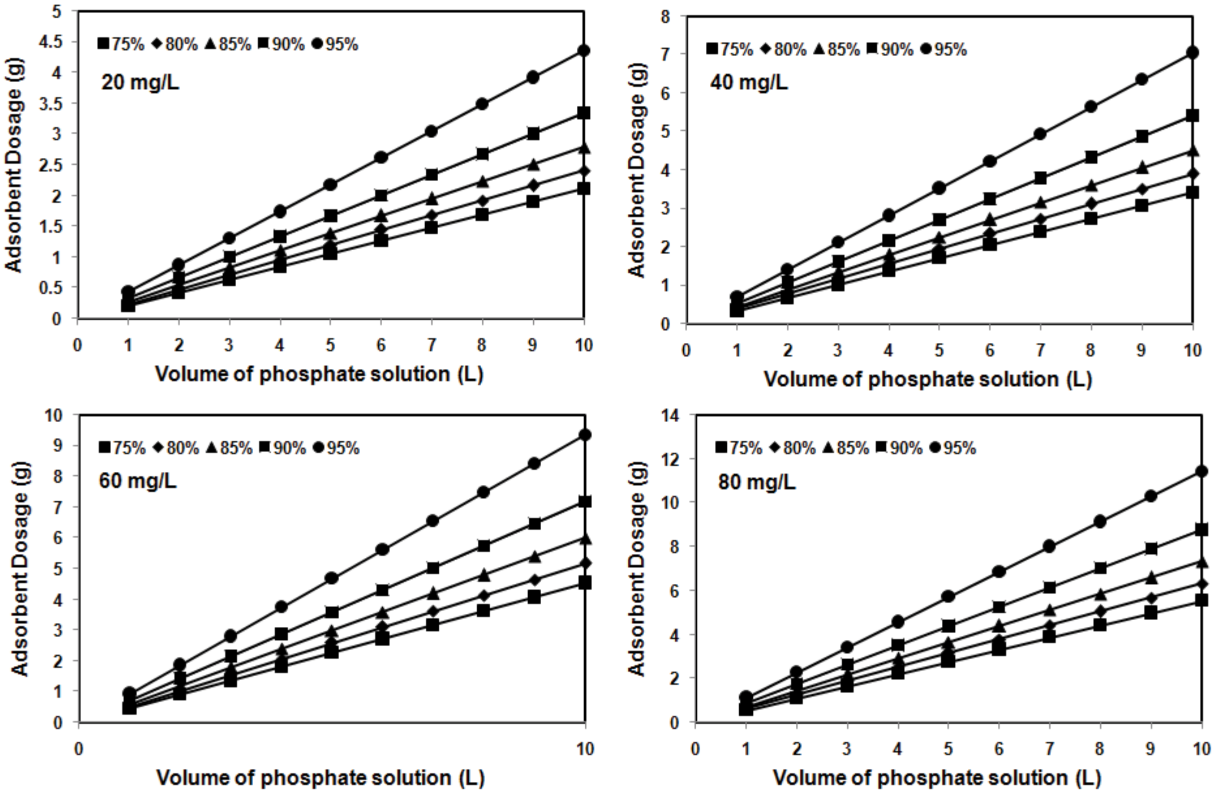

Fig. 13 (Continued)

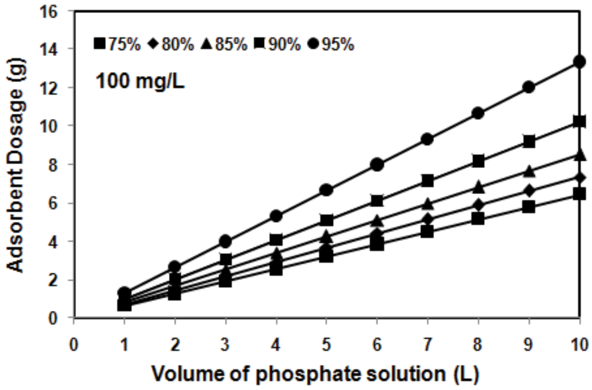

Fig. 13. Batch adsorber design on the elimination of phosphates by HTC.

4. Conclusion

The current study's goal was to eliminate P and N using the sugarcane waste acquired from a locally run juice shop in Chennai. HTC carbon sphere works well as an adsorbent to take phosphate and nitrate out of water. It was discovered that the starting concentration, contact duration, solution pH, temperature, and adsorbent dose all affected the quantity of P and N that was adsorbed. A successful percentage of P and N ion elimination was observed at the following optimal conditions: pH 7.0, 1,400 mg/L of adsorbent, 1 h of contact time, and a temperature of 303 K. According to isotherm investigations, the Freundlich equation, which explains the multi-layer adsorption behavior that was essentially the sorption of the P and N ions on HTC carbon sphere, was the best isotherm framework for the elimination of P and N ions. At 30°C, the produced adsorbent had a maximum P and N adsorption capacity of 91.23 and 60.96 mg/g, accordingly. Entropy, enthalpy, and Gibbs free energy thermodynamic variables' negative values imply that spontaneous, exothermic, and thermodynamically viable phosphate and nitrate ion sorption on HTC carbon sphere is achievable at reduced temperatures. The adsorption rate was discovered to have the greatest correlation coefficient and to follow pseudo-first-order kinetics. It was discovered that pore diffusion regulated the overall rate of dye absorption, but the plots showed that this mechanism was not the only one that determined rate. For the removal of P and N by HTC carbon spheres, utilizing the Langmuir model, a one stage batch design was proposed. This work reveals that cheap biomaterials, such as HTC carbon spheres made of sugarcane bagasse, can serve as an alternative to numerous expensive adsorbents used to remove P and N from wastewater.

Conflicts of interest statement

Authors declare that no conflicts of interest for this article. No copyediting or translation services were used for the preparation of this manuscript.

Symbols

C_{ae} — Intensity of N and P attached to the carbon spheres at equilibrium condition
C_e — Intensity at saturation condition
T — Temperature
k_C — Equilibrium constant
R — Universal gas constant
q_e — Amount of N and P adsorbed at any time
C_o — Initial concentration of N and P in aqueous solution
V — Volume of aqueous solution used
W_{sorbent} — Mass of the adsorbent
q_m — Maximum capacity for a single layer of absorption
K_L — Langmuir constant, L/mg
K_F — Freundlich constant
b_t, a_t — Temkin isotherm constants
q_t — Amount of P and N ion stored at a certain time on carbon spheres
C_t — Concentration of P and N ion at any interval of time
k_1, k_2 — First and second-order sorption rate constant
α — Adsorption rate constant
β — Desorption rate constant.
k_p — Intraparticle diffusion constant
m — Mass of the adsorbent
n — Freundlich exponent

References

[1] S. Hamoudi, R. Saad, K. Belkacemi, Adsorptive removal of phosphate and nitrate anions from aqueous solutions using ammonium-functionalized mesoporous silica, Ind. Eng. Chem. Res., 46 (2007) 8806–8812.

[2] T.K.M. Prashantha Kumar, T.R. Mandlimath, P. Sangeetha, S.K. Revathi, A.S.K. Kumar, Nanoscale materials as sorbents for nitrate and phosphate removal from water, Environ. Chem. Lett., 16 (2018) 389–400.

[3] P. Karthikeyan, H.A.T. Banu, S. Meenakshi, Removal of phosphate and nitrate ions from aqueous solution using La^{3+} incorporated chitosan biopolymeric matrix membrane, Int. J. Biol. Macromol., 124 (2019) 492–504.

[4] A.S. Eltaweil, A.M. Omer, H.G. El-Aqapa, N.M. Gaber, N.F. Attia, G.M. El-Subruiti, E.M. Abd El-Monaem, Chitosan based adsorbents for the removal of phosphate and nitrate: a critical review, Carbohydr. Polym., 274 (2021) 118671, doi: 10.1016/j.carbpol.2021.118671.

[5] B. Wu, J. Wan, Y. Zhang, B. Pan, I.M. Lo, Selective phosphate removal from water and wastewater using sorption: process

fundamentals and removal mechanisms, Environ. Sci. Technol., 54 (2019) 50–66.

[6] C.V. Lazaratou, D.V. Vayenas, D. Papoulis, The role of clays, clay minerals and clay-based materials for nitrate removal from water systems: a review, Appl. Clay Sci., 185 (2020) 105377, doi: 10.1016/j.clay.2019.105377.

[7] K. Velusamy, S. Periyasamy, P.S. Kumar, D.V.N. Vo, J. Sindhu, D. Sneka, B. Subhashini, Advanced techniques to remove phosphates and nitrates from waters: a review, Environ. Chem. Lett.,19 (2021) 3165–3180.

[8] M. Zhang, G. Song, D.L. Gelardi, L. Huang, E. Khan, O. Mašek, Y.S. Ok, Evaluating biochar and its modifications for the removal of ammonium, nitrate, and phosphate in water, Water Res., 186 (2020) 116303, doi: 10.1016/j.watres.2020.116303.

[9] K.M.S. Khalil, M. Khairy, O.A.S. Allam, M.K. Khalil, Formation of improved activated carbons from sugarcane bagasse as environmental materials for adsorption of phenolic pollutants, Int. J. Environ. Sci. Technol., 19 (2022) 3103–3116.

[10] H. Tian, J. Liang, J. Liu, Nanoengineering carbon spheres as nanoreactors for sustainable energy applications, Adv. Mater., 31 (2019) 1903886, doi: Nanoengineering carbon spheres as nanoreactors for sustainable energy applications.

[11] Z.C. Wang, X. Cai, K. Li, Y.Y. Ye, Z.X. Zhang, Y.Q. Liu, D. Wang, S.R. Li, LiBr hydrate as reaction medium for preparation of carbon spheres from wood powders via hydrothermal carbonization, Diamond Relat. Mater., 113 (2021) 108295, doi: 10.1016/j.diamond.2021.108295.

[12] G. Prasannamedha, P.S. Kumar, Hydrothermal carbonization of waste sugarcane bagasse for the effective removal of emerging contaminants from aqueous solution, Adsorpt. Sci. Technol., 2022 (2022) 1–13.

[13] B. Hu, K. Wang, L. Wu, S.H. Yu, M. Antonietti, M.M. Titirici, Engineering carbon materials from the hydrothermal carbonization process of biomass, Adv. Mater., 22 (2010) 813–828.

[14] L. Wang, Y. Chang, A. Li, Hydrothermal carbonization for energy-efficient processing of sewage sludge: a review, Renewable Sustainable Energy Rev., 108 (2019) 423–440.

[15] N.D. Berge, K.S. Ro, J. Mao, J.R. Flora, M.A. Chappell, S. Bae, Hydrothermal carbonization of municipal waste streams, Environ. Sci. Technol., 45 (2011) 5696–5703.

[16] Y. Shen, A review on hydrothermal carbonization of biomass and plastic wastes to energy products, Biomass Bioenergy, 134 (2020) 105479, doi: 10.1016/j.biombioe.2020.105479.

[17] M. Sevilla, A.B. Fuertes, The production of carbon materials by hydrothermal carbonization of cellulose, Carbon, 47 (2009) 2281–2289.

[18] A. Funke, F. Ziegler, Hydrothermal carbonization of biomass: a summary and discussion of chemical mechanisms for process engineering, Biofuel Bioprod. Biorefin., 4 (2010) 160–177.

[19] D. Congsomjit, C. Areeprasert, Hydrochar-derived activated carbon from sugar cane bagasse employing hydrothermal carbonization and steam activation for syrup decolorization, Biomass Convers. Biorefin., 11 (2021) 2569–2584.

[20] M.M. Titirici, M. Antonietti, Chemistry and materials options of sustainable carbon materials made by hydrothermal carbonization, Chem. Soc. Rev., 39 (2010) 103–116.

[21] G. Prasannamedha, P.S. Kumar, R. Mehala, T.J. Sharumitha, D. Surendhar, Enhanced adsorptive removal of sulfamethoxazole from water using biochar derived from hydrothermal carbonization of sugarcane bagasse, J. Hazard. Mater., 407 (2021) 124825, doi: 10.1016/j.jhazmat.2020.124825.

[22] W.J. Weber Jr., J.C. Morris, Kinetics of adsorption on carbon from solution, J. Sanit. Eng. Div., 89 (1963) 31–59.

[23] S. Basu, G. Ghosh, S. Saha, Adsorption characteristics of phosphoric acid induced activation of bio-carbon: equilibrium, kinetics, thermodynamics and batch adsorber design, Process Saf. Environ. Prot., 117 (2018) 125–142.

[24] Y.W. Berkessa, S.T. Mereta, F.F. Feyisa, Simultaneous removal of nitrate and phosphate from wastewater using solid waste from factory, Appl. Water Sci., 9 (2019) 1–10.

[25] B.S. Rathi, P.S. Kumar, R. Ponprasath, K. Rohan, N. Jahnavi, An effective separation of toxic arsenic from aquatic environment using electrochemical ion exchange process, J. Hazard. Mater., 412 (2021) 125240, doi: 10.1016/j.jhazmat.2021.125240.

[26] P.S. Kumar, S. Ramalingam, S.D. Kirupha, A. Murugesan, T. Vidhyadevi, S. Sivanesan, Adsorption behavior of nickel(II) onto cashew nutshell: equilibrium, thermodynamics, kinetics, mechanism and process design, Chem. Eng. J., 167 (2011) 122–131.

[27] I. Langmuir, The adsorption of gases on plane surfaces of glass, mica and platinum, J. Am. Chem. Soc., 40 (1918) 1361–1403.

[28] H. Freundlich, Adsorption in solution, Phys. Chem. Soc., 40 (1906) 1361–1368.

[29] R.D. Johnson, F.H. Arnold, The Temkin isotherm describes heterogeneous protein adsorption, Biochim. Biophys. Acta, Protein Struct. Mol. Enzymol., 1247 (1995) 293–297.

[30] S.K. Lagergren, About the theory of so-called adsorption of soluble substances, Sven. Vetenskapsakad. Handingarl, 24 (1898) 1–39.

[31] Y.S. Ho, G. McKay, Pseudo-second-order model for sorption processes, Process Biochem., 34 (1999) 451–465.

[32] S.H. Chien, W.R. Clayton, Application of Elovich equation to the kinetics of phosphate release and sorption in soils, Soil Sci. Soc. Am. J., 44 (1980) 265–268.

[33] O. Alagha, M.S. Manzar, M. Zubair, I. Anil, N.D. Mu'azu, A. Qureshi, Comparative adsorptive removal of phosphate and nitrate from wastewater using biochar-MgAl LDH nanocomposites: coexisting anions effect and mechanistic studies, Nanomaterials, 10 (2020) 336, doi: 10.3390/nano10020336.

[34] P. Karthikeyan, S. Meenakshi, Synthesis and characterization of Zn-Al LDHs/activated carbon composite and its adsorption properties for phosphate and nitrate ions in aqueous medium, J. Mol. Liq., 296 (2019) 111766, doi: 10.1016/j.molliq.2019.111766.

[35] A. Olgun, N. Atar, S. Wang, Batch and column studies of phosphate and nitrate adsorption on waste solids containing boron impurity, Chem. Eng. J., 222 (2013) 108–119.

[36] Y. Shao, J. Li, X. Fang, Z. Yang, Y. Qu, M. Yang, W. Tan, G. Li, H. Wang, Chemical modification of bamboo activated carbon surface and its adsorption property of simultaneous removal of phosphate and nitrate, Chemosphere, 287 (2022) 132118, doi: 10.1016/j.chemosphere.2021.132118.